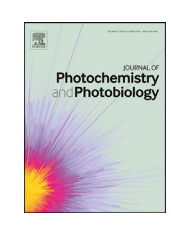


Contents lists available at ScienceDirect

Journal of Photochemistry and Photobiology

journal homepage: www.elsevier.com/locate/jpap



Excited state proton transfer dye with an emission quantum yield up to 60% upon Zn^{2+} coordination



Suliman Ayad, Tanmay Banerjee, Bryan Casale, Erica S. Knorr, Kenneth Hanson*

Department of Chemistry & Biochemistry, Florida State University, Tallahassee, Florida 32306, USA

ARTICLE INFO

Keywords: Sensor Zinc ESIPT BPI Hydrazine

ABSTRACT

Intramolecular excited state proton transfer (ESIPT) dyes are appealing for metal ion sensing because of their large apparent Stokes-shift, environmental sensitivity, and turn-on fluorescence capabilities. Here we introduce 1,3-bis(2-pyridylimino)-4,7-dihydroxyisoindole (2) as a new ESIPT sensing motif. The 2,5-bis(2-pyridylimino)pyrrole portion of 2 readily coordinates Hg^{2+} , Zn^{2+} , Zn^{2+} , Zn^{2+} , and Zn^{2+} ions and results in a visible red-shift in absorption. While coordination of Zn^{2+} and Zn^{2+} and Zn^{2+} increases the ESIPT emission quantum yield from 25% to 60%. Unlike traditional ESIPT sensors, the metal ion binding site of 2 is intrinsic to the chromophore but is not the ESIPT site, thus enabling the selective modification of each functionality. As proof of concept, we use bromobutyrate as an alcohol protecting group whose cleavage by hydrazine results in turn-on fluorescence response. Collectively these results demonstrate the 1,3-bis(2-pyridylimino)-4,7-dihydroxyisoindole motif is sensitive to several stimuli (i.e. metal ion, base, solvent, and Zn^{2}) and is a promising scaffolding for sensing applications.

1. Introduction

Colorimetric and fluorometric metal ion sensors are useful for a range of applications from biological labelling [1] to detecting heavy metal contamination in the environment [2,3]. In the presence of the targeted analyte, these sensors typically exhibit a turn-on/-off emission and/or a discernible spectral shift in absorption/emission. Given these requirements, excited state intramolecular proton transfer (ESIPT) dyes are a particularly appealing class of molecular sensors because they are highly sensitive to environmental changes (e.g. solvent, pH, etc.) and exhibit large apparent Stokes shifts [4-6]. ESIPT compounds for sensing metal ions typically employ either 1) a 'fluorophore spacer receptor' architecture where the metal ion chelator and the chromo/fluorophoric unit are covalently linked in proximity but are largely independent moieties [7-9] or 2) the ESIPT functional groups can directly serve as the metal ion binding site where the proton is replaced by a metal ion [10]. Alternatively, one can envision an ESIPT dye where the metal ion chelator is intrinsic to the chromophore, but not the ESIPT site, which may provide a means of retaining ESIPT emission but with increased sensitivity and amplified spectral response to the analyte.

In 2011, Hanson et al. reported 1,3-bis(2-pyridylimino)-4,7-dihydroxyisoindole (2 in Figure 1) as a new class of ESIPT dye [10]. Photoexcitation of this molecule leads to an electron density shift away from the phenolic protons (OH) and toward the imine (N) followed by

excited state proton transfer from O to N, and finally emission from the proton transferred, keto state [11,12]. Compound 2 exhibits a large apparent stokes shift (>6,000 cm⁻¹) and an ESIPT emission quantum yields of >30% [11]. The latter is particularly notable in that it is one of the highest ESIPT quantum yields reported to date [4,5]. Equally important, at least for the present study, is that compound 2 contains a 1,3-bis(2-pyridylimino)isoindole core which is a tridentate, monoanionic ligand known for binding a large range of metal ions like Fe²⁺, Co²⁺, Ni²⁺, Cu²⁺, Zn²⁺, Cd²⁺, and more [13–17]. Therefore, unlike typical ESIPT metal ion sensors [18,19], the metal ion binding site in 2 is conjugated to the photoactive portion of the dye and may be directly involved in influencing the ESIPT event. Herein we report our study into the influence of metal(II) ions on the photophysical properties of 1,3-bis(2-pyridylimino)-4,7-dihydroxyisoindole-based ESIPT dyes. Our experiments show that this ESIPT dye is responsive to several metal ions but a more than two-fold enhancement in emission quantum yield upon coordination with Zn2+ ions. Additionally, we demonstrate that with the use of phenolic protecting groups, this dye can also serve as turn-on fluorescence probe for hydrazine.

2. Materials and Methods

Barium perchlorate, calcium perchlorate tetrahydrate, calcium chloride, cadmium perchlorate hydrate, cobalt(II) perchlorate hexahy-

E-mail address: hanson@chem.fsu.edu (K. Hanson).

^{*} Corresponding author.

1: R, R' = H

2: R, R' = OH

3: R = OH, R' = Boc

4: R = BrButyrate, R' = Boc

Fig. 1. Structure of molecules 1-4 and the proposed coordination site of the M^{2+} ions.

drate, copper(II) perchlorate hexahydrate, iron(II) perchlorate hydrate, mercury(II) perchlorate hydrate, magnesium perchlorate hexahydrate, manganese(II) perchlorate hydrate, nickel(II) perchlorate hexahydrate, zinc perchlorate hexahydrate, cadmium acetate dihydrate, copper(II) acetate, sodium acetate trihydrate, 2-aminopyridine, 2,3-dicyanohydroquinone, 4-(dimethylamino)pyridine (DMAP), 1-Ethyl-3-(3-dimethylaminopropyl)carbodiimide hydrochloride (EDC HCl), ditert-butyl dicarbonate (Boc₂O), and 4-bromobutanoic acid, n-butanol, acetonitrile, dichloromethane, toluene, and methanol were all purchased from Sigma Aldrich and used without further purification. Sodium chloride (Ward's Scientific), dimethyl sulfoxide, strontium perchlorate trihydrate, zinc acetate dihydrate (Alpha Aesar), and ethylene glycol (EMD Millipore) were purchased from their respective suppliers, in parentheses, and used without further purification. Compounds 1 [20] and 2 [10] were synthesized following previously published procedure.

Synthesis of 3: 2 (500 mg, 1.5 mmol), di-tert-butyl dicarbonate (489 mg, 2.24 mmol) and dimethylaminopyridine (DMAP) (182 mg, 1.5 mmol) were added to a 250 mL three neck round bottom flask equipped with a magnetic stir bar and dissolved in acetonitrile (100 mL). The flask was purged and backfilled with $\rm N_2$ three times and stirred at room temperature. The reaction progress was monitored by TLC. After 2 days the solvent was evaporated in vacuo and the crude mixture was purified by column chromatography on silica gel using a 10% ethylacetate in hexanes mobile phase. The fractions were combined and evaporated to dryness to obtain 3 (0.417 g, 65% yield) as a yellow amorphous solid. $^1\rm H$ NMR (400 MHz, DMSO- $^4\rm d_6$) δ 13.89 (s, 1H), 8.73 (dddd, J = 8.7, 4.9, 1.9, 0.9 Hz, 2H), 8.01–7.89 (m, 2H), 7.61–7.54 (m, 1H), 7.38 (ddd, J = 7.9, 5.5, 1.0 Hz, 2H), 7.34–7.26 (m, 2H), 7.19 (dd, J = 8.7, 0.9 Hz, 1H), 1.50 (s, 9H). DART-HRMS: m/z calcd. For $\rm C_{23}\rm H_{21}\rm N_5\rm O_4$ ([M+H]+) 432.1627, found 432.1681

Synthesis of 4: 3 (100 mg, 0.23 mmol), 4-bromobutanoic acid (50 mL, 0.48 mmol), 1-Ethyl-3-(3-dimethylaminopropyl)carbodiimide HCl (EDC) (114 mg, 0.59 mmol), and DMAP (15.8 mg, 0.13 mmol) were added to a 100 mL three neck round bottom flask equipped with a magnetic stir bar and dissolved in dichloromethane (50 mL). The flask was purged and backfilled with N2 three times and stirred at room temperature. Reaction progress was monitored by disappearance of orange emission, which is indicative of the alcohol's protection. Once orange emission completely disappeared (~3 days), the reaction was quenched with 25 mL H₂O. The reaction crude was extracted three times with DCM then concentrated in vaccuo. The crude material was recrystallized from DCM by layering with hexanes. The crystals were filtered, rinsed with hexanes, then dried in vaccuo to yield 4 (0.102 g, 78% yield) as a pale yellow crystalline solid. ¹H NMR (400 MHz, DMSO- d_6) δ 14.18 (s, 1H), 8.81-8.67 (m, 2H), 7.95 (dtd, J = 11.7, 7.5, 1.9 Hz, 2H), 7.66-7.49(m, 2H), 7.42 (d, J = 8.1 Hz, 1H), 7.38 (d, J = 8.1 Hz, 1H), 7.31 (ddt, J = 7.5, 4.9, 1.3 Hz, 2H), 3.72 (t, J = 6.5 Hz, 2H), 3.00 (t, J = 7.4 Hz, 2H), 2.27 (m, J = 6.9 Hz, 2H), 1.50 (s, 9H). DART-HRMS: m/z calcd. For $\rm C_{27}H_{26}N_5O_5Br~([M+H]^+)~580.1151$ and 582.1131, found 580.1208 and 582.1191.

Instrumentation: Absorption (Agilent 8453), steady-state and time resolved emission (Edinburgh FLS980), quantum yield (Hamamatsu Quantaurus), NMR (Bruker), and HR-MS (Agilent 6200 Q-TOF-MS coupled to an IonSense DART SVP) measurements were performed on commercially available instrumentation with experimental details provided in the supporting information.

3. Results and Discussion

3.1. Synthesis

The chromophores/fluorophores used in this study are shown in Fig. 1. The parent, non-ESIPT dye 1 (a.k.a. BPI), was synthesized using the alkaline-earth-catalyzed nucleophilic addition of pyridyl amine to 1,2-dicyanobenzene in butanol as originally reported by Siegl [20]. Compound 2 was synthesized using the same procedure but with minor modifications as described previously (Scheme 1) [10]. It is worth mentioning that the reaction time (20 days) and yield (20%) for 2 were notably lower and longer than 1 (2 days and 68%) presumably due to deactivation of the cyano groups by the alcohol substituents. Attempts to increase the reaction rate by refluxing in ethylene glycol (bp: 198°C versus 118°C for n-butanol) resulted in a markedly shortened reaction time from ~20 days to 2 h as determined by the disappearance of starting material. However, concomitant with the formation of 2 was a yellow emitting side product, which was difficult to separate by column chromatography and only a small portion of the desired product was isolated (4% yield). Longer reaction times (~8 h) in ethylene glycol led to the complete decomposition of 2 as evidenced by TLC.

Using ultrafast spectroscopy, Dawlaty and coworkers demonstrated that one alcohol group of 2 is sufficient for ESIPT to occur [21,22]. With this in mind, we prepared compounds 3 and 4 containing a single Boc (i.e. *tert*butoxycarbonyl), and both Boc and bromo butyrate phenolic protecting groups, respectively. These were selected as the alcohol protecting groups because 1) Boc increases the solubility of 2 and 2) bromo butyrate is known to undergo cleavage in the presence of hydrazine enabling "turn-on" fluorescence sensing (*vide infra*) [23–25]. Compound 3 was synthesized by reacting 2 with di-*tert*-butyl dicarbonate anhydride in acetonitrile to give 3 in 65% yield. Interestingly, even with a large excess of di-tert-butyl dicarbonate anhydride, Boc addition only occurred at one of the OH groups of making this a convenient strategy for asymmetric functionalization of 2. Subsequent reaction of 3 with 4-bromobutyric acid in DCM in the presence of EDC and with DMAP catalyst gave compound 4 in 78% yield [26].

3.2. Metal Ion Chelation

The photophysical properties of 1 and 2 in the absence and presence of metal(II) perchlorate salts was measured in a 90:10 mixture of DMSO/water (v/v). Due to the low solubility of 1 and 2 in aqueous conditions, DMSO was selected as the primary solvent for photophysical studies. However, with the intention of creating a practical methodology (i.e. sampling aqueous biological fluids), 10% volume of water or water containing the cations of interest were added to 1 or 2 in DMSO. It is important to note that there was negligible change in the absorption and emission spectra (Figure S1) or the excited state lifetime (Figure S2) of 2 in DMSO after the addition of 10% water.

The parent molecule 1, with no OH groups for proton transfer, exhibits highly structured absorption features at <420 nm and only had a negligible blue emission ($\Phi_{em} < 0.01\%$) at room temperature. In contrast, 2 has less well defined, but still structured absorption (350–480 nm), bright orange emission at 610 nm ($\Phi_{em} = 25\%$), and a large apparent Stokes shift (6,600 cm⁻¹) consistent with absorption in the enol state, ESIPT, and then emission from the keto state [10].

Scheme 1. Synthesis of compounds 2, 3, and 4.

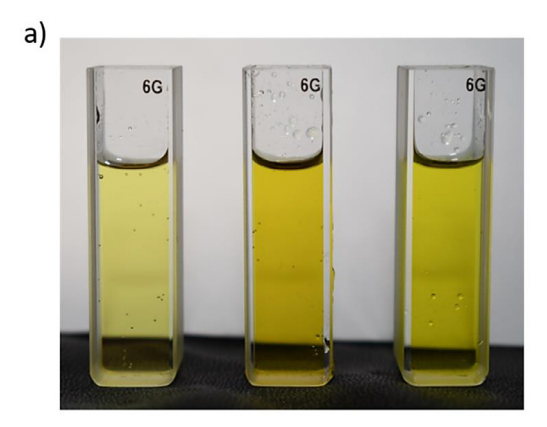
Fig. 2. Normalized absorption spectra of 1 (a) and 2 (b) without and with 100 equivalents of Hg^{2+} , Zn^{2+} , and Ni^{2+} . (c) Emission spectra for 2 without and with 100 equivalents Zn^{2+} ($\lambda_{ex} = 400$ nm). All spectra were acquired in DMSO with 10% H_2O (v/v) and $\sim 5 \times 10^{-7}$ M dye concentration.

Select absorption and emission spectra of 1 and 2 following the addition of 100 equivalents of dication perchlorate salts are shown in Fig. 2 with the remaining spectra provided in supporting information (Figure S3). The addition of Ba^{2+} , Ca^{2+} , Cd^{2+} , Fe^{2+} , Mg^{2+} , Mn^{2+} , and Sr^{2+} to 1 had minimal effect on the absorption spectra (Figure S3a). The most observable change in this series was in the amplitude, but not position, of the high energy absorption peaks upon the addition of Fe^{2+} however this can be attributed to increased light scattering from the relatively insoluble Fe(II) salt. The lack of spectral shifts suggests that either the ions are coordinating but have no influence, or far more likely is that these metal ions do not coordinate to 1 under these conditions.

In contrast, notable bathochromic shifts in absorption (Fig. 2a and Figure S3b) can be observed upon the addition of Hg^{2+} , Zn^{2+} , Co^{2+} , and Cu^{2+} with the largest shift for Ni^{2+} (0.33 eV). While most retain the vibrational structure, there is significant broadening in the presence of Hg^{2+} the origin of which is currently unclear to us. For these metal ions, we attribute the spectral shift to metal ion coordination to the 2,5-bis(2-pyridylimino)pyrrole portion of the molecule which effectively pulls electron density away from the π -system and lowers the energy of the π - π * transition. The absence of absorption from the parent 1 and complete shift in the spectra indicates that for these cations, there is irreversible and/or at least heavily coordination favoured metal ion binding to the dye under these conditions. It is important to note that despite metal ion coordination to 1, no emission enhancement was observed from these complexes ($\Phi_{\rm em} < 0.01\%$).

For the absorption spectra of complex 2 in the presence of dications, similar trends were observed as with 1. That is, a nominal shift in absorption or emission with Ba²⁺, Ca²⁺, Cd²⁺, Fe²⁺, Mg²⁺, Mn²⁺, and Sr²⁺ (Figure S3c) but bathochromic shifts in absorption with Hg²⁺, Zn²⁺, Co²⁺, Cu²⁺, and Ni²⁺ (Fig. 2b and Figure S3d). The trend and the magnitude of the shift were similar to as with 1, which lacks the OH group, suggesting that metal ion coordination to 2 is at the 2,5-bis(2pyridylimino)pyrrole portion of the molecule and not the ESIPT site (i.e. OH—N). Interestingly, for Co²⁺ there is a small but discernible, low energy, structured absorption features from 500-620 nm (Fig. 3b). Similar spectral features was observed in 5,6-dichloro-1,3-bis(2-pyridylimino)-4,7-dihydroxyisoindole [10] and can be attributed to absorption from the keto form of molecule (i.e. O- and NH form). This observation is important in that it indicates that metal ion coordination is an effective means of perturbing the enol-keto equilibrium even in the ground state of the 1,3-bis(2-pyridylimino)-4,7-dihydroxyisoindole dye. While relatively weak, at sufficiently high concentrations this feature combined with the spectral shift results in a color change of 2 upon addition of Hg²⁺ and Co²⁺ (Fig. 3a) making it an intriguing candidate for colorimetric sensing.

The cation coordination also influences the emissive behaviour of 2 and the results are summarized in Fig. 2c and Table S1. As with absorption, the non-coordinating cations had minimal influence on the energy ($\lambda_{em} \approx 610$ nm), lifetime ($\tau \approx 3.5$ ns) or quantum yield ($\Phi_{em} \approx 25\%$) of emission from 2 (Table S1). On the other hand, coordination with



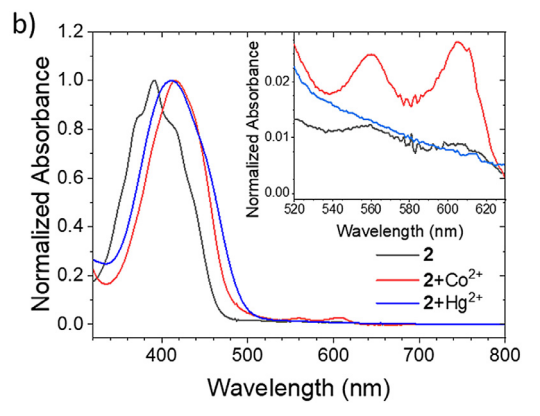


Fig. 3. a) Photograph of solutions containing 1 mM solutions of 2 (left), 2 with 10 equivalents of $\mathrm{Co^{2+}}$ (middle), and 2 with 10 equivalents of $\mathrm{Hg^{2+}}$ (right) perchlorate salts in DMSO with $\mathrm{10\%}$ H₂O (v/v) under ambient light and b) absorption spectra of the same solutions after \sim 20 fold dilution (inset: zoom of the normalized absorption spectra between 520 and 630 nm).

 Co^{2+} , Cu^{2+} , Hg^{2+} , and Ni^{2+} completely quenched emission from 2 ($\Phi_{em} < 0.01\%$). While we have not definitively established a mechanism, excited state quenching by these ions is not unusual and is often attributed to either excited state electron transfer or paramagnetic quenching [27–29].

Remarkably, coordination of $\rm Zn^{2+}$ (Zn-2) not only shifted the enolemission peak to 630 nm (Fig. 2c) but also increased the excited state lifetime ($\tau=4.1$ ns) and more than doubled the emission quantum yield ($\Phi_{\rm em}=60\%$) of 2. The emission enhancement can be attributed to both a decrease in the non-radiative decay rate constant ($k_{nr}=2.4\times10^8~{\rm s^{-1}}$) and a two-fold increase in the radiative decay rate constant ($k_r=1.5\times10^8~{\rm s^{-1}}$) of Zn-2 relative to 2 ($k_{nr}=3.2\times10^8~{\rm s^{-1}}$). In terms of non-radiative decay, one can envision metal ion coordination increasing the rigidity of the molecule and inhibiting vibrational relaxation modes. Regardless of the mechanism, the spectral shift and increase emission intensity are sufficiently large to visually differentiate the sample with and without $\rm Zn^{2+}$ ions (Fig. 4).

3.3. Zn-2 Coordination Chemistry

Previous reports indicate that Zn^{2+} can coordinate to BPI in either tetrahedral [17] or octahedral [30] geometries. Given the remarkable enhancement in photophysical properties, we sought to gain structural insights into the Zn-2 adduct observed here. Unfortunately, all attempts to grow crystals of the Zn-2 were unsuccessful (see SI for more details). Instead, we monitored changes in the 1H NMR spectrum of 2 in DMSO- d_6 upon the addition of Zn^{2+} ions and the results can be seen in Fig. 5. In the absence of Zn^{2+} , compound 2 exhibits five well defined peaks from 7.0–9.0 ppm indicating a plane of symmetry bisecting the isoindole portion

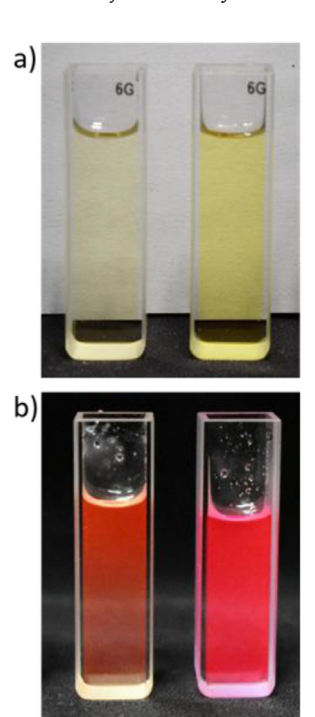


Fig. 4. Photograph of solutions containing 2 in DMSO with $10\%~H_2O~(v/v)$ without (left) and with (right) 100 equivalents of Zn^{2+} under (a) ambient light and (b) UV irradiation.

of the molecule. The peak assignments for this region, four from the pyridyl ring (H_{b-e}) and one from the isoindole (H_a), are shown in Fig. 5.

Upon the addition of $Zn(ClO_4)_2$ there is a decrease in the NMR peaks associated with 2 and a concurrent increase in an equal number but shifted peaks for Zn-2. While the indole proton (H_a) remained largely unaffected, there are notable upfield and downfield shifts for H_e and H_{b-d} (Fig. 5) that are accompanied by the disappearance of the H_f , isoindoline proton at 13.7 ppm (Figure S4). These changes are consistent with previous reports of Zn^{2+} coordination to the 2,5-bis(2-pyridylimino)pyrrolate portion of the molecule [17,30] and not the ES-IPT site. The lack of symmetry breaking that was observed with the tetrahedral Zn-BPI complex reported by Anderson et al.[17] suggests 2 is binding Zn^{2+} via a tridentate and octahedral coordination environment [30].

To investigate the binding stoichiometry of 2 with $\rm Zn^{2+}$ we employed the method of continuous variations, also known as a Job plot, as has been previously reported with other metal ion probes [31–33]. Here we monitored the absorption spectral changes with respect to the molar ratio of $\rm Zn^{2+}$ and the normalized absorption spectra are shown in Figure S5 [31,34]. The Job plot was then generated by graphing the absorption changes at 443 nm (i.e. the distinct absorption feature for Zn-2, see Fig. 2b) versus the mole fraction of $\rm Zn^{2+}$ and the results are shown in Fig. 6. The peak maximum at \sim 0.33 as well as the sigmoidal shape of the graph at higher mole fractions are indicative of an $\rm AB_2$ binding motif [31].

Collectively these results indicate that Zn^{2+} is octahedrally coordinated at the 2,5-bis(2-pyridylimino)pyrrolate site of 2 with a stoichiometry of $Zn(2)_2$. Similar coordination chemistry was proposed by Gagne et al for $Zn(4,4'-dimethylBPI)_2$ [30].

3.4. Effects of Solvent, Salt, and pH

To probe the environmental effects, we measured the photophysical properties of 2 with variation in solvent (DMSO, MeOH, and MeOD), pH (with and without NaOAc), and $\rm Zn^{2+}$ salt ($\rm Zn(ClO_4)_2$, and $\rm Zn(OAc)_2$) and the results are summarized in Table 1 with the spectra in Figure S6.

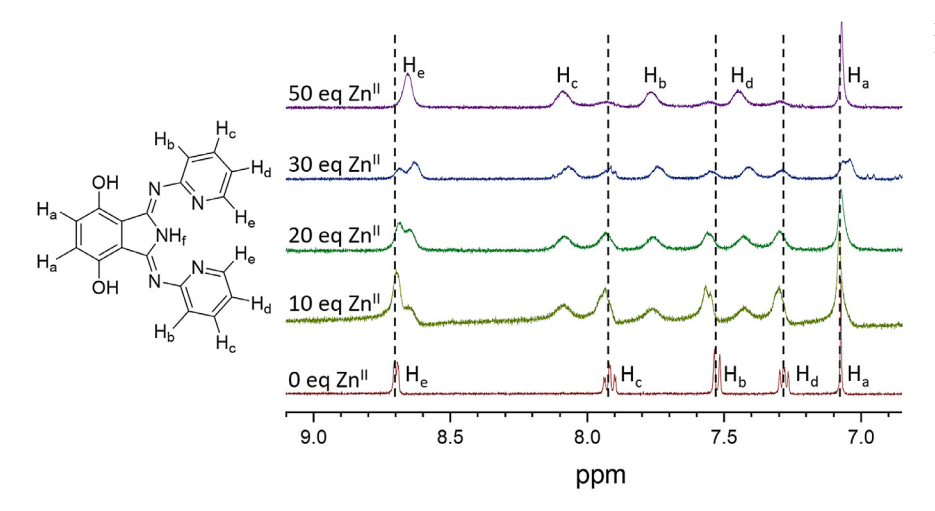


Figure 5. 1 H NMR spectra of 2 in DMSO- d_{6} during a titration with 0 to 50 equivalents of $Zn(ClO_{4})_{2}$.

Table 1 Photophysical properties of 2 with variation in solvent, pH, and counter ions.

Entry	Solvent	Salt ^a	Absorption (nm)	Emission at rt ^b				
				λ_{max} (nm)	τ (ns)	Φ_{PL}	$k_r (\times 10^8 \text{s}^{-1})^{\text{c}}$	$k_{nr} (\times 10^8 \text{s}^{-1})^{\text{d}}$
1	DMSO	-	390	616	3.0	0.25	0.8	3.3
2	DMSO	NaOAc	350, 605	616	6.3	0.12	0.2	1.6
3	DMSO	$Zn(ClO_4)_2$	417	630	4.1	0.60	1.5	2.4
4	DMSO	$Zn(OAc)_2$	405, 605	630	8.0	0.68	0.9	1.2
5	MeOH	- ' '	385, 590	594	3.8	0.23	0.6	2.6
6	MeOH	NaOAc	385, 590	596	3.9	0.09	0.2	2.6
7	MeOH	$Zn(ClO_4)_2$	413, 590	606	4.3	0.28	0.6	2.3
8	MeOH	$Zn(OAc)_2$	398, 560	615	8.8	0.48	0.5	1.1
9	MeOD	-	385, 590	592	6.7	0.11	0.2	1.5
10	MeOD	NaOAc	385, 590	595	6.8	0.23	0.3	1.5
11	MeOD	$Zn(ClO_4)_2$	385, 540	615	8.2	0.10	0.1	1.2
12	MeOD	$Zn(OAc)_2$	398, 560	617	10.4	0.34	0.3	1.0

^a 100 equivalents of each salt relative to 2.

^b Emission data acquired using dilute solutions ($\sim 5 \times 10^{-7}$ M (c) $k_{\rm r} = \Phi/\tau$. (d) $k_{\rm nr} = (1-\Phi)/\tau$.

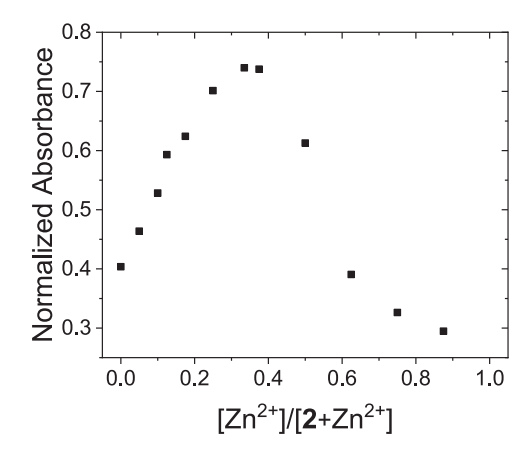


Fig. 6. Job plot of the absorbance at 443 nm for 2 with varying molar ratios of $\rm Zn^{2+}$ in DMSO. The total concentration of 2 and $\rm Zn^{2+}$ was maintained at 0.05 mM.

In line with the results above, upon the addition of $\rm Zn(ClO_4)_2$ to 2 in DMSO (entry 3 in Table 1), there is a red-shift in absorption and emission as well as an increase in both the excited state lifetime and emission quantum yield relative to 2 alone (entry 1). For both solutions there are no notable absorption features below 500 nm. In contrast, the addition of acetate, as either NaOAc or $\rm Zn(OAc)_2$, results in a dramatic increase in the absorption peak at 605 nm. Presumably, the acetate makes the solution sufficiently basic as to deprotonate the ESIPT site and increase

the "keto" character of ground state 2 and Zn-2. Interestingly, the addition of acetate also decreases the radiative and non-radiative decay rate constants.

In both methanol (entry 5–8) and deuterated methanol (entry 9–12) the low energy absorption feature is weakly present in 2 and Zn-2 solutions but again is dramatically enhanced upon the addition of acetate. Relative to that in DMSO there is also a general increase in excited state lifetime but decrease in emission quantum yield that can be attributed to the lower radiative rate in MeOH and MeOD. In agreement with previous studies [35,36], deuteration (MeOD) of the ESIPT dyes increases the excited state lifetime and decreases the non-radiative decay relative to the protonated dye (MeOH).

Not surprisingly these results demonstrate the high sensitivity of 2 to solvent and pH effects. But regardless of solvent, there was a general trend of increasing emission quantum yield and lifetime upon $\rm Zn^{2+}$ coordination to 2 which was further enhanced by the addition of acetate. The higher pH also increases the contribution of the low energy "keto" absorption feature, but these effects could readily be reversed by the addition of acetic acid (Figure S7).

3.5. Deprotection by Hydrazine

Analyte induced cleavage of a protecting group on the proton donor site of an ESIPT dyes is an appealing strategy to realize turn-on fluorescence detection of species like H_2S ,[26,37] O_2^- ,[38] ONOO, $^-$ [39] and hydrazine [25]. The latter is of particular interest because hydrazine is an acutely toxic and carcinogenic compound [40,41] that is commonly used in many industrial, agricultural, and pharmaceutical pro-

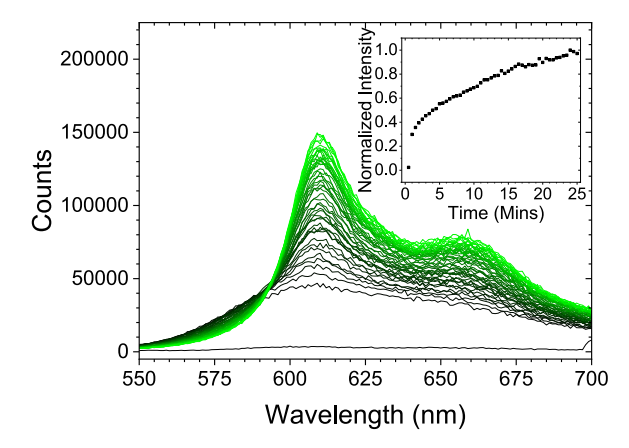


Fig. 7. Emission spectra changes of 4 with respect to time after the addition of 2.2 equivalents of N_2H_4 (black to green, spectra acquired every 0.5 min). Inset: Emission intensity at 610 nm with respect to time. ($\lambda_{ex} = 390$ nm)

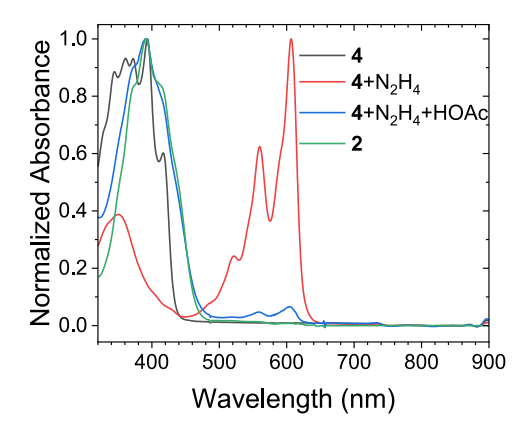


Fig. 8. Absorption spectra of 4 in DMSO before and after the addition of 2.2 equivalents of N_2H_4 and then the addition of excess HOAc. The spectrum of 2 in DMSO is included for reference.

cesses [42]. As previously demonstrated by Goswami et al., a bromobutyrate alcohol protecting group is readily cleaved in the presence of hydrazine resulting in turn-on fluorescence [25]. To further expand the detection capabilities of 2, we generated the compounds 3 and 4 containing a single Boc, and both Boc and bromobutyrate phenolic protecting groups, respectively.

The similarity in photophysical properties between 2 and 3 is not surprising because it has previously been demonstrated that one alcohol group of 2 is sufficient for ESIPT to occur (Figure S8) [21,22]. However, the addition of both Boc and bromobutyrate phenolic protecting groups to 2 results in compound 4 whose photophysical properties more closely resemble non-emissive 1 ($\Phi_{em} < 0.01\%$). This behaviour can be rationalized by the lack of OH donor for the ESIPT process to occur which prevents keto emission that is observed in 2 and 3. At time 0 (i.e. prior to N_2H_4 addition) no emission was observed. However, immediately after the introduction of N_2H_4 , bright red emission was readily apparent, even to the naked eye. The emission intensity continued to increase until plateauing at ~20 min after the initial addition. The emission spectra are consistent with the keto-type emission that is observed with 2 and 3 (Fig. 7).

Following completion of the reaction, the solution was quenched with dilute HCl. The absorption spectrum of the product (Fig. 8) resembles that of 2 treated with NaOAc (Figure S6a) suggesting that the hydrazine is not only capable of cleaving both protecting groups of 4 but is also sufficiently basic to deprotonate the product. This hypothesis is further supported by the addition of excess acetic acid to the $4+N_2H_4$ solution where the spectrum of the acidified product most closely re-

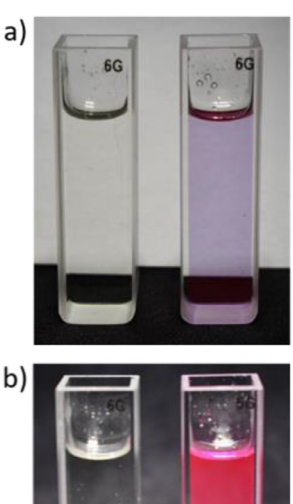




Fig. 9. Photograph of 4 in DMSO without (left) and with (right) N_2H_4 under (a) ambient light and (b) UV irradiation.

sembles that of fully protonated 2 (Fig. 8), and not the Boc protected molecule 3.

Collectively this indicates that 4 does exhibit turn-on fluorescence in the presence of $\rm N_2H_4$. However, it is not by enabling an ESIPT mechanism but instead by the $\rm N_2H_4$ induced generation of the deprotonated form of 2 followed by excitation and emission from the keto form of the molecule. Presumably, performing the hydrazine reaction in a sufficiently acidic medium would result in the "direct" formation of 2 and the typical large apparent Stokes shifted emission. Nonetheless, the dramatic change in both absorption and emission spectra of 4 in DMSO upon the addition of $\rm N_2H_4$, makes this a promising colorimetric and fluorometric probe for the detection of hydrazine (Fig. 9).

It is worth noting that from the UV-Vis and emission measurements, the same metal ion interactions described above in section 3.2 and 3.3 for 1 and 2, are also active in molecules 3 and 4. While not explored here, this indicates that different combinations of metal ion, hydrazine, and molecule 4 will result in unique spectral signatures (i.e. turn-on fluorescence, absorption/emission shifts, etc.) which could open the door to complex, multicomponent detection schemes.

4. Conclusions

Here we introduce the ESIPT dye, 1,3-bis(2-pyridylimino)-4,7-dihydroxyisoindole (2) as a new sensing motif for both transition metal ions and hydrazine. Cations like Ba²⁺, Ca²⁺, Cd²⁺, Fe²⁺, Mg²⁺, Mn²⁺, and Sr²⁺ have minimal influence on the photophysical properties of 2 but the addition of Hg²⁺, Zn²⁺, Co²⁺, Cu²⁺, and Ni²⁺results in a distinct red shift in absorption with Hg²⁺, Co²⁺, Ni²⁺, and Cu²⁺ completely quenching emission from 2. In contrast, Zn²⁺ coordination resulted in a more than two-fold enhancement in emission quantum yield from 25% to 60% which is due to a decrease and increase in non-radiative and radiative rates, respectively. Similarly, in all solvents tested (ie. DMSO, MeOH, and MeOD) there was a general trend of increasing emission quantum yield and lifetime upon Zn²⁺ coordination to 2 which was further enhanced by the addition of base. Comparative measurements to 1,3-bis(2-pyridylimino)-isoindole indicate that the transition metal ions coordinate to the 2,5-bis(2-pyridylimino)pyrrole portion of 2 and not

the ESIPT site. NMR measurements and the Job plot suggest that tridentate coordination of 2 to Zn^{2+} results in an octahedral complex with $\mathrm{Zn}(2)_2$ stoichiometry. Additionally, with the appropriate alcohol protecting groups, the 1,3-bis(2-pyridylimino)-4,7-dihydroxyisoindole motif can serve as a fluorescence turn-on sensor for $\mathrm{N}_2\mathrm{H}_4$.

Collectively these results demonstrate that 1,3-bis(2-pyridylimino)-4,7-dihydroxyisoindole exhibits a distinct colorimetric and fluorometric response to several stimuli (i.e. metal ion, base, solvent, and N_2H_4) and is a promising motif for sensing applications. With that said, the current molecule shows minimal sensitivity and selectivity for any particular transition metal ion. Presumably by varying the steric and electronic properties of the 2,5-bis(2-pyridylimino)pyrrole metal ion binding site, one could increase the selectivity. This combined with the one step synthesis makes this a versatile and promising motif for a number of sensing applications.

Declaration of Competing Interest

The authors declare that they have no known competing financial interests or personal relationships that could have appeared to influence the work reported in this paper.

Acknowledgements

The authors would like to thank the Florida State University and the Energy & Materials Initiative for facilitating aspects of this research. Photophysical measurements were supported by the National Science Foundation under Grant No. DMR-1752782. A portion of these measurements were conducted in the FSU Department of Chemistry and Biochemistry's NMR (FSU075000NMR), Mass Spec (FSU075000MASS), and Materials Characterization (FSU075000MAC) Laboratories.

Supplementary materials

Supplementary material associated with this article can be found, in the online version, at doi:10.1016/j.jpap.2021.100029.

References

- K.P. Carter, A.M. Young, A.E. Palmer, Fluorescent sensors for measuring metal ions in living systems, Chem Rev 114 (2014) 4564–4601, doi:10.1021/cr400546e.
- [2] N. De Acha, C. Elosúa, J.M. Corres, F.J. Arregui, Fluorescent sensors for the detection of heavy metal ions in aqueous media, Sensors 19 (2019) 599, doi:10.3390/s19030599
- [3] L. Feng, H. Li, L.-Y. Niu, Y.-S. Guan, C.-F. Duan, Y.-F. Guan, C.-H. Tung, Q.-Z. Yang, A fluorometric paper-based sensor array for the discrimination of heavy-metal ions, Talanta 108 (2013) 103–108, doi:10.1016/j.talanta.2013.02.073.
- [4] X. Liu, A. Li, W. Xu, Z. Ma, X. Jia, An ESIPT-based fluorescent switch with AIEE, solvatochromism, mechanochromism and photochromism, Mater. Chem. Front. 4 (2019) 620–625, doi:10.1039/C8QM00633D.
- [5] Seo Jangwon, a. Sehoon Kim, S.Y. Park, Strong solvatochromic fluorescence from the intramolecular charge-transfer state created by excited-state intramolecular proton transfer, J. Am. Chem. Soc. 126 (2004) 11154–11155, doi:10.1021/ja047815i.
- [6] J. Zhao, S. Ji, Y. Chen, H. Guo, P. Yang, Excited state intramolecular proton transfer (ESIPT): from principal photophysics to the development of new chromophores and applications in fluorescent molecular probes and luminescent materials, PCCP 14 (2012) 8803–8817, doi:10.1039/C2CP23144A.
- [7] Kaur, B.; Kaur, N.; Kumar, S., Colorimetric metal ion sensors: a comprehensive review of the years 2011-2016. Coordination Chemistry Reviews2017, 358, 13–69. https://doi.org/10.1016/j.ccr.2017.12.002.
- [8] W.-H. Chen, Y. Xing, Y. Pang, A highly selective pyrophosphate sensor based on ESIPT turn-on in water, Org. Lett. 13 (2011) 1362–1365, doi:10.1021/ol200054w.
- [9] A.P.d. Silva, T.S. Moody, G.D. Wright, Fluorescent PET (Photoinduced Electron Transfer) sensors as potent analytical tools, Analyst 134 (2009) 2385–2393, doi:10.1039/B912527M.
- [10] K. Hanson, N. Patel, M.T. Whited, P.I. Djurovich, M.E. Thompson, Substituted 1,3-Bis(imino)isoindole Diols: a new class of proton transfer dyes, Org. Lett. 13 (2011) 1598–1601, doi:10.1021/ol103106m.
- [11] C. Ma, Y. Yang, C. Li, Y. Liu, TD-DFT study of the double excited-state intramolecular proton transfer mechanism of 1,3-Bis(2-pyridylimino)-4,7-dihydroxyisoindole, J. Phys. Chem. A 119 (2015) 12686–12692, doi:10.1021/acs.jpca.5b09430.
- [12] S. Kataria, L. Rhyman, P. Ramasami, N. Sekar, Comprehensive DFT and TD-DFT Studies on the Photophysical Properties of 5,6-Dichloro-1,3-Bis(2-Pyridylimino)-4,7-Dihydroxyisoindole: a new class of ESIPT fluorophore, J. Fluoresc. 26 (2016) 18051812, doi:10.1007/s10895-016-1872-6.

- [13] R. Csonka, G. Speier, J. Kaizer, Isoindoline-derived ligands and applications, RSC Adv. 5 (2015) 18401–18419. doi:10.1039/C4RA15379K.
- [14] D.C. Sauer, R.L. Melen, M. Kruck, L.H. Gade, Chromophores, fluorophores and robust ancillary ligands for molecular catalysts: 1,3-Bis(2-pyridylimino)isoindolines, Eur. J. Inorg. Chem. 2014 (2014) 4715, doi:10.1002/ejic.201402798.
- [15] K. Hanson, L. Roskop, N. Patel, L. Griffe, P.I. Djurovich, M.S. Gordon, M.E. Thompson, Photophysical and electrochemical properties of 1,3-bis(2-pyridylimino)isoindolate platinum(ii) derivatives, Dalton Trans. 41 (2012) 8648–8659, doi:10.1039/C2DT30354J.
- [16] K. Hanson, L. Roskop, P.I. Djurovich, F. Zahariev, M.S. Gordon, M.E. Thompson, A paradigm for blue- or red-shifted absorption of small molecules depending on the site of π-extension, J. Am. Chem. Soc. 132 (2010) 16247–16255, doi:10.1021/ja1075162.
- [17] Anderson, O. P.; la Cour, A.; Dodd, A.; Garrett, A. D.; Wicholas, M., Syntheses and structures of isoindoline complexes of Zn(II) and Cu(II): an unexpected Trinuclear Zn(II) Complex. *Inorganic Chemistry* 2003, 42, 122–127. https://doi.org/10.1021/jc011246n.
- [18] W.-H. Chen, Y. Xing, Y. Pang, A highly selective pyrophosphate sensor based on ESIPT turn-on in water, Org. Lett. 13 (2011) 1362–1365, doi:10.1021/ol200054w.
- [19] Y. Xu, Y. Pang, Zn 2+ -triggered excited-state intramolecular proton transfer: a sensitive probe with near-infrared emission from bis(benzoxazole) derivative, Dalton Trans. 40 (2011) 1503–1509, doi:10.1039/C0DT01376E.
- [20] W.O. Siegl, Metal ion activation of nitriles. Syntheses of 1,3-bis(arylimino)isoindolines, J. Org. Chem. 42 (1977) 1872–1878, doi:10.1021/jo00431a011.
- [21] E. Driscoll, S. Sorenson, J.M. Dawlaty, Ultrafast intramolecular electron and proton transfer in Bis(imino)isoindole Derivatives, J. Phys. Chem. A 119 (2015) 5618–5625, doi:10.1021/acs.jpca.5b02889.
- [22] R. Welsch, E. Driscoll, J.M. Dawlaty, T.F. Miller, Molecular Seesaw: how increased hydrogen bonding can hinder excited-state proton transfer, J. Phys. Chem. Lett. 7 (2016) 3616–3620, doi:10.1021/acs.jpclett.6b01391.
- [23] Y. Hao, Y. Zhang, K. Ruan, W. Chen, B. Zhou, X. Tan, Y. Wang, L. Zhao, G. Zhang, P. Qu, M. Xu, A naphthalimide-based chemodosimetric probe for ratiometric detection of hydrazine, Sens. Actuators B 244 (2017) 417–424, doi:10.1016/j.snb.2016.12.145.
- [24] S. Goswami, K. Aich, S. Das, S. Basu Roy, B. Pakhira, S. Sarkar, A reaction based colorimetric as well as fluorescence 'turn on' probe for the rapid detection of hydrazine, RSC Adv. 4 (2014) 14210–14214, doi:10.1039/C3RA46663A.
- [25] S. Goswami, S. Das, K. Aich, B. Pakhira, S. Panja, S.K. Mukherjee, S. Sarkar, A chemodosimeter for the ratiometric detection of hydrazine based on return of ESIPT and its application in live-cell imaging, Org. Lett. 15 (2013) 5412–5415, doi:10.1021/014026759.
- [26] S.I. Reja, N. Sharma, M. Gupta, P. Bajaj, V. Bhalla, R.D. Parihar, P. Ohri, G. Kaur, M. Kumar, A highly selective fluorescent probe for detection of hydrogen sulfide in living systems: in vitro and in vivo applications, Chem. Eur. J. 23 (2017) 9872–9878, doi:10.1002/chem.201701124.
- [27] R.W. Ricci, K.B. Kilichowski, Fluorescence quenching of the indole ring system by lanthanide ions, J. Phys. Chem. 78 (1974) 1953–1956, doi:10.1021/j100612a017.
- [28] P. Yuster, S.I. Weissman, Effects of perturbations on phosphorescence: luminescence of metal organic complexes, J. Chem. Phys. 17 (1949) 1182–1188, doi:10.1063/1.1747140.
- [29] D.M. Guldi, T.D. Mody, N.N. Gerasimchuk, D. Magda, J.L. Sessler, Influence of large metal cations on the photophysical properties of texaphyrin, a rigid aromatic chromophore, J. Am. Chem. Soc. 122 (2000) 8289–8298, doi:10.1021/ja001578b.
- [30] Gagne, R. R.; Marritt, W. A.; Marks, D. N.; Siegl, W. O., Mononuclear and binuclear metal complexes of 1,3-bis(2-pyridylimino)isoindolines. *Inorganic Chemistry*1981, 20, 3260–3267. https://doi.org/10.1021/ic50224a024.
- [31] J.S. Renny, L.L. Tomasevich, E.H. Tallmadge, D.B. Collum, Method of continuous variations: applications of job plots to the study of molecular associations in organometallic chemistry, Angew Chem Int Ed Engl 52 (2013) 11998–12013, doi:10.1002/anie.201304157.
- [32] B. Xue-Jiao, R. Jing, Z. Jia, S. Zhi-Bin, A 'turn-on' fluorescent chemosensor for the detection of Zn2+ ion based on 2-(quinolin-2-yl)quinazolin-4(3H)-one, Heterocycl. Commun. 24 (2018) 135–139, doi:10.1515/hc-2017-0136.
- [33] R.Q. Paulpandi, S. Ramasamy, M.S. Paulraj, F.G. Díaz Baños, G. Villora, J.P. Cerón-Carrasco, H. Pérez-Sánchez, I.V. Muthu Vijayan Enoch, Enhanced Zn2+ ion-sensing behavior of a benzothiazole derivative on encapsulation by β-cyclodextrin, RSC Adv. 6 (2016) 15670–15677, doi:10.1039/C6RA01202G.
- [34] M. Mabrouk, S.F. Hammad, M.A. Abdelaziz, F.R. Mansour, Ligand exchange method for determination of mole ratios of relatively weak metal complexes: a comparative study, Chem. Cent. J. 12 (2018) 143, doi:10.1186/s13065-018-0512-4.
- [35] A.J.G. Strandjord, P.F. Barbara, Hydrogen/deuterium isotope effects on the excited-state proton transfer kinetics of 3-hydroxyflavone, Chem. Phys. Lett. 98 (1) (1983) 21–26, doi:10.1016/0009-2614(83)80194-8.
- [36] N.B. Aein, P. Wan, Excited state intramolecular proton transfer (ESIPT) from phenol OH (OD) to adjacent "aromatic" carbons in simple biphenyls, J. Photochem. Photobiol. A 208 (2009) 42–49, doi:10.1016/j.jphotochem.2009.08.004.
- [37] W. Chen, S. Chen, B. Zhou, H. Wang, X. Song, H. Zhang, Highly selective red-emitting H2S fluorescent probe with a large Stokes shift, Dyes Pigm. 113 (2015) 596–601, doi:10.1016/j.dyepig.2014.09.035.
- [38] D.P. Murale, H. Kim, W.S. Choi, D.G. Churchill, Highly selective Excited State Intramolecular Proton Transfer (ESIPT)-based superoxide probing, Org. Lett. 15 (2013) 3946–3949, doi:10.1021/ol4017222.
- [39] X. Li, R.-R. Tao, L.-J. Hong, J. Cheng, Q. Jiang, Y.-M. Lu, M.-H. Liao, W.-F. Ye, N.-N. Lu, F. Han, Y.-Z. Hu, Y.-H. Hu, Visualizing peroxynitrite fluxes in endothelial cells reveals the dynamic progression of brain vascular injury, J. Am. Chem. Soc. 137 (2015) 12296–12303, doi:10.1021/jacs.5b06865.

- [40] CT Liverman, I. C., C.E. Fulco, et al., The National Library of Medicine's Toxicology and Environmental Health Information Program editors, National Academies Press
- [41] Garrod Sarah, Mary E. Bollard, Andrew W. Nicholls, Susan C. Connor, John Connelly, Jeremy K. Nicholson, a., Elaine Holmes, Integrated metabonomic analysis of the
- multiorgan effects of hydrazine toxicity in the rat, Chem. Res. Toxicol. 18 (2005) 115–122, doi:10.1021/tx0498915.

 [42] U. Ragnarsson, Synthetic methodology for alkyl substituted hydrazines, Chem. Soc. Rev. 30 (2001) 205–213, doi:10.1039/B010091A.